Chemosphere 287 (2022) 132394

Contents lists available at ScienceDirect

Chemosphere

journal homepage: www.elsevier.com/locate/chemosphere

Transformation products of the high-volume production chemicals 1-vinyl-2-pyrrolidinone and 2-piperazin-1-ylethanamine formed by UV photolysis

Benigno José Sieira, Rosario Rodil *, Rafael Cela, José Benito Quintana **, Rosa Montes ***

Department of Analytical Chemistry, Institute of Research on Chemical and Biological Analysis (IAQBUS), Universidade de Santiago de Compostela, Santiago de Compostela, 15782, Spain

HIGHLIGHTS

- VP and PPE are high-volume, highly reactive, production chemicals.
- Twelve TPs identified after UV irradiation.
- Uncertain toxicity estimations were made by QSARs.
- Experimental investigations of toxicity needed.

GRAPHICAL ABSTRACT

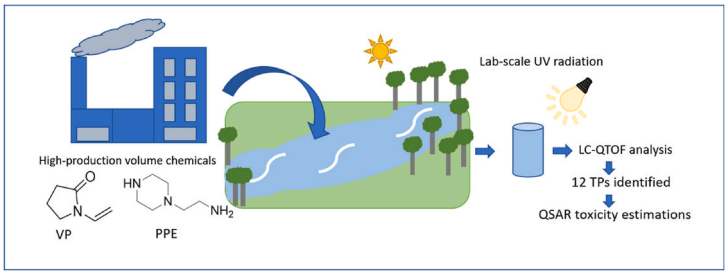

ARTICLE INFO

Handling Editor: Jun Huang

Keywords:
PMOCs
PMT chemicals
Photodegradation
High resolution mass spectrometry

ABSTRACT

This work investigates the reaction of 1-vinyl-2-pyrrolidinone (VP) and 2-piperazin-1-yletanamine (PPE) under UV radiation. Both substances are high-volume production chemicals (production >1000 tons/year) widely used in polymers, coatings and a wide array of applications, which have been classified as mobile chemicals and which can then lead to the formation of persistent and mobile transformation products (TPs). Thus, their reaction with UV light was studied by means of liquid chromatography-quadrupole-time-of-flight-mass spectrometry (LC-QTOF-MS). Both compounds presented a high reactivity, the VP quantum yield was 0.28 mol/E; whereas, PPE had a quantum yield notably higher than 1 (16 mol/E). Five and 7 TPs were identified for VP and PPE, respectively. Some of them had been already reported in literature due to sunlight photodegradation or other oxidation processes, but most of them are reported here for the first time. Finally, the acute and chronical toxicity of precursors and TPs were estimated using two quantitative structure-activity relationship (QSAR) software tools which led to some discrepancies in the estimations, pointing to the need for experimental toxicity assays for these compounds.

* Corresponding author.
** Corresponding author.
*** Corresponding author.
E-mail addresses: rosario.rodil@usc.es (R. Rodil), jb.quintana@usc.es (J.B. Quintana), rosamaria.montes@usc.es (R. Montes).

https://doi.org/10.1016/j.chemosphere.2021.132394
Received 24 May 2021; Received in revised form 7 September 2021; Accepted 26 September 2021
Available online 27 September 2021

1. Introduction

Persistent and mobile organic compounds (PMOCs) are chemical substances whose presence in the environment has recently generated concern (Reemtsma et al., 2016). This terminology refers to compounds with high polarity and therefore, water solubility, that can easily break through the different barriers and spread across the water cycle. If, in addition, these compounds present certain toxicity, the concern becomes even greater and they could be classified as persistent and mobile (and potentially toxic) substances (PM(T) substances) (Neumann, 2017). This last terminology was used in a parallelism to the PBT (persistent, bioaccumulative and toxic) criteria used by REACH to classify compounds as substances of very high concern (SVHC) and highlight the need for a similar legislative treatment for potentially toxic PMOCs since they could represent an equivalent level of concern (Hale et al., 2020). The increasing interest on PMOCs/PMT compounds has led to the development of dedicated analytical methodology, capable of reporting qualitative (Gago-Ferrero et al., 2015; Montes et al., 2017; Schymanski et al., 2014) and quantitative (Bieber et al., 2017; Montes et al., 2019) data on their presence in the environment.

Natural and anthropogenic processes that take place in nature, wastewater treatment plants (WWTP) or drinking water facilities can lead to the formation of transformation products (TPs) with similar or even higher polarity or toxicity than their precursor compounds, consequently increasing the list of substances of potential concern (Bletsou et al., 2015). Thus, such potential TPs have been included in suspect screening strategies through the elaboration of databases based on computer-aided (in-silico) prediction tools, commercially available or freely accessible, such as University of Minnesota Pathway Prediction System (UM-PPS) (Kern et al., 2009) or Meteor (http://www.lhasalimited.org/products/meteor-nexus.htm), respectively. On the other hand, lab-scale approaches can be performed for target pollutants of concern through the simulation of the transformation processes in batch experiments with the parent compound submitted to biodegradation, chlorination, photolysis, etc. (Carpinteiro et al., 2017; González-Mariño et al., 2018; Helbling et al., 2010; Sieira et al., 2020), which enable the identification of TPs.

The number of compounds that can be potentially classified as PMOCs or PMOC-TPs is extremely high and therefore prioritization approaches must be performed to select compounds which degradation or occurrence need further investigation (European Environment Agency, 2019). In this sense, some authors (Arp et al., 2017; Schulze et al., 2018) proposed a PMOCs prioritization strategy based on the mobility, persistency and emission data of high production volume substances registered under REACH. From the resulting list (Schulze et al., 2018), Zahn et al. (2019) selected a subset of 11 environmental relevant substances on the basis of their standard availability, liquid chromatography-mass spectrometry (LC-MS) amenability and novelty and performed stability test based on hydrolysis, photolysis, MnO_2 oxidation, and biotransformation processes. The evaluation of the results of Zahn et al. (2019) suggested that further study of the TP of two PMOCs under UV radiation would be of interest. These chemicals are 1-vinyl-2-pyrrolidinone (VP) and 2-piperazin-1-yletanamine (PPE). VP is the monomer of the widely deployed polymer polyvinylpyrrolidone and otherwise used in washing and cleaning products with a registered production higher than 1000 tonnes/year in the EU (ECHA, 2011). The European Chemicals Bureau report of risk assessment for this compound (European Chemicals Bureau, 2003) published a predicted environmental concentration lower than 50 μg/L even for contaminated surface water, however, more recently, concentrations in the mg per litre level have been already found in river and wastewater samples (Antić et al., 2011). PPE is used in adhesives and sealants, coating products, paints and polymers with a registered production of 1000–10,000 tonnes/year (ECHA, 2010). This compound have been found in surface water samples in a previous work involving different analytical strategies, although with a relatively low (14%) frequency of detection (Schulze et al., 2019).

Hence, the aims of this study were to delve into the transformation of VP and PPE under UV radiation including a kinetic study, to identify the TPs by LC-HRMS, and to conduct a preliminary (eco)toxicological assessment.

2. Materials and methods

2.1. Chemicals and stock solutions

VP and PPE properties and structure information are compiled in Table S1. Commercial standards of both compounds, as well as diclofenac (DCF) were purchased from Sigma-Aldrich (Milwaukee, WI, USA). Stock solutions (ca. 1000 mg/L) were prepared in ultra-pure water for further dilutions.

Ultra-pure water (18.2 MΩ cm) was obtained directly from the lab from a Milli-Q Gradient A-10 system (Millipore, Bedform, MA, USA). Acetonitrile (ACN) and methanol (MeOH), both in LC-MS grade, were purchased from Merck (Darmstadt, Germany).

2.2. Real samples

Besides ultrapure water, a river (Sarela river, Santiago de Compostela, Spain) sample (pH 6.5, dissolved organic carbon (DOC): 8.7 mg/L, bromide: 0.035 mg/L; UV254: 5.95×10^{-2}) was collected in amber bottles and stored at 4 °C until used during a maximum period of 48 h. Before photolysis experiments, the sample was filtered through 0.45 μm nitrocellulose filters (Millipore) to remove particle matter.

2.3. Photolysis experiments

Photodegradation experiments were performed in 30 mm o. d. diameter quartz tubes (Afora, Barcelona, Spain) containing 25 mL of ultra-pure water or river water. UV photodegradation was carried out using a homemade photoreactor equipped with two 8-W low-pressure Hg lamps (Philips reference G8 T5) emitting at 254 nm, a fan to dissipate the heat and an orifice to introduce the quartz tube perpendicularly to the lamps. Further details on the design can be found elsewhere (Castro et al., 2016; González-Mariño et al., 2018). The flux density of radiation was measured using potassium iodide as actinometer. The measured value was 7.2 mW/cm^2 (González-Mariño et al., 2018). Lamps were equilibrated for 30 min before starting any test.

A preliminary study to determine the stability of VP and PPE chemicals was done in 25 mL of ultra-pure (pH 5.8) and river water (pH 6.5) by using 2 mg/L of either each of them or DCF. Different aliquots of 1 mL were taken at different times between 0 and 60 min to estimate the photochemical degradation kinetic and rate constant in both kinds of samples. River water samples were filtered through a 0.22 μm PVDF syringe filters (Merck-Millipore, Bedford, MA, USA) before HPLC analysis. A dark control was also performed in an oven at 40 °C for 60 min.

The experiments for TP identification were performed in ultra-pure water at higher concentrations of precursors (20 mg/L) to improve the detectability of such TPs. In some experiments, ethanol (HPLC grade from Merck) was also added (50 μM) as an •OH radicals scavenger (Hu et al., 2012).

2.4. LC-HRMS

Samples were analyzed on an LC-QTOF-MS system consisting of an Agilent 1200 Series (Agilent Technologies, Santa Clara, CA, USA) LC equipped with a degasser, a binary high-pressure pump, LC column oven and an autosampler, which was hyphenated to an Agilent 6520 Series QTOF MS furnished with a Dual Electrospray (Dual-ESI) ion source.

The LC column used in this work was a Luna C18-2 (Phenomenex, 150 mm × 2.1 mm; 3 μm). The mobile phase flow was 0.2 mL/min and the column temperature 35 °C. The injection volume was set at 10 μL.

The binary gradient was programmed as follows: 0 min, 5% B; 10 min, 100% B; 12 min, 100% B; 12.10 min, 5% B; 23 min, 5% B. Eluents A and B consisted of water and methanol, respectively, both containing 0.1% formic acid.

Nitrogen (99.9%), used as nebulising and drying gas in the QTOF, was supplied by a nitrogen generator (Erre Due Srl, Livorno, Italy). Collision-Induced Dissociation (CID) for the tandem mass spectrometry analysis (MS/MS) was performed with Nitrogen (99.9995%) purchased from Praxair (Santiago de Compostela, Spain). The ESI source was operated in positive polarity (ESI+), since no TPs were detected in negative mode, with source parameters set as follows: gas temperature 350 °C; drying gas flow 5 L/min; nebulizer pressure 42 psig, capillary 4000 V; fragmentor 120 V; skimmer 65 V; and octapole RF 750 V. Instrument acquired MS spectra in centroid and was operated in the 2 GHz (extended-dynamic range) mode, which provided a Full Width at Half Maximum (FWHM) resolution of ca. 4500 at m/z 121.0509 and ca. 11000 at m/z 922.0098. A reference solution prepared according to the manufacturer specifications was continuously infused during every run through the secondary sprayer of the Dual-ESI at 5 psig, to automatically recalibrate and maintain mass accuracy. The masses, *m/z* 121.0509 and 922.0098, from this solution were used for this recalibration.

Data analysis was performed with the MassHunter Qualitative Analysis software (Agilent Technologies). The response of the chemicals tested as well as the TPs tentatively identified was performed by integrating the area of the peaks on the narrow-window (20 ppm) extracted ion chromatograms (EIC) of the $[M+H]^+$ ion. Identification of the TPs was initiated by the peak-picking algorithm "Find by Molecular Feature" with an area threshold of 1000 counts. The features obtained were exported as CEF files and further analyzed on the MassProfiler Professional software (Agilent Technologies), for peak alignment and statistical analysis, where peaks increasing as regards to the "time 0" reference constitute putative TPs, as detailed elsewhere (Carpinteiro et al., 2017). Then, formulas were generated by stabilising a score threshold of 80 and a maximum mass error of 5 ppm.

Finally, those putative TPs were subjected to a subsequent injection by target tandem mass spectrometry (MS/MS) for structural elucidation, considering three collision energies (10, 20 and 40 V).

2.5. Ecotoxicological prediction

To estimate the ecotoxicity of VP and PPE and their transformation products, two QSAR software were used, the US EPA T.E.S.T. version 4.1 and ECOSAR version 1.11. In T.E.S.T. software, the 48-h *Daphnia magna* LC_{50}, 96-h *Fathead minnow* LC_{50}, 48-h *Tetrahymena pyriformis* IGC_{50} and oral rat LD_{50} endpoints were estimated by the consensus method, which uses an average value of the calculated toxicities by five different QSAR methodologies (Carpinteiro et al., 2017). On the other hand, in ECOSAR, the 48-h *Daphnia magna* LC_{50}, 96-h fish LC_{50}, 96-h green algae EC_{50} and chronic toxicity values (ChV) for the same species were estimated (Carpinteiro et al., 2017).

3. Results and discussion

3.1. Photochemical reactivity

After irradiation of ultra-pure water samples for up to 60 min, both VP and PPE reacted significantly, presenting half-lives of 1.9 and 40 min, respectively. Similar kinetic constants were obtained in river water samples (Fig. S1 and Table S2). The pH and temperatures of both types of samples was measured before and after irradiation. No changes in the pH were observed after the 60 min irradiation period, while the temperature increased from 22 °C to 32 °C. In the dark control, no changes in the concentrations of VP and PPE were observed. VP is a neutral chemical, while PPE is a basic compound with several amino groups. According to its predicted pK_a values, under typical environmental pH values (4–8), it would be present as dicationic species (protonated in the secondary and primary amine groups) (Chemicalize, 2021).

DCF, a pharmaceutical with several studies on its photochemical kinetics, produced a half-life of 1.4 min (Table S2). Since data on the quantum yield (Φ) of DCF at 254 nm has already been published (Wols and Hofman-Caris, 2012), it could be employed as a chemical actinometer, in order to calculate the value of Φ for VP and PPE, according to the following equation (Eq. (1)) (González-Mariño et al., 2018; Weidauer et al., 2016):

$$\Phi_{chem} = \Phi_{DCF} \times \frac{k_{d(chem)}}{k_{d(DCF)}} \times \frac{\varepsilon_{254(DCF)}\, I_{0,254}}{\varepsilon_{254(chem)} I_{0,254}} \quad (1)$$

where Φ_{chem} and Φ_{DCF} are the quantum yields, $k_{d(chem)}$ and $k_{d(DCF)}$ are the direct photolysis rate constants (min^{-1}), $\varepsilon_{254(chem)}$ and $\varepsilon_{254(DCF)}$ the molar absorption coefficients at 254 nm and $I_{0,254}$ is the intensity of the lamp, which emits almost exclusively at 254 nm; *chem* refers to the chemical whose quantum yield is calculated and DCF is the selected chemical actinometer. The values of ε were determined experimentally using 1 cm path-length quartz cuvettes and are compiled in Table S2. VP quantum yield was 0.28 mol/E, whereas PPE had a quantum yield notably higher than 1 (16 mol/E). Such a high UV reactivity was unexpected in the case of PPE, given its weak absorption in the UV region. However, PPE has been proven also to be reactive to solar radiation (Zahn et al., 2019), which is also not expected given its UV–visible spectrum (Fig. S2). In the publication of Zahn et al. (2019) this solar photochemical activity was ascribed to the formation of singlet oxygen, since the reaction did not take place in absence of oxygen or presence of furfuryl alcohol. When the photochemical reaction was performed in the presence of ethanol, an •OH radical scavenger (Hu et al., 2012), the reaction was partially quenched: 32 ± 3% Vs. 56 ± 4% PPE remaining after 1 h irradiation in absence or presence of ethanol, respectively. Thus, generation of •OH radicals and other species from oxygen may be related to such photochemical reactivity (Ryu et al., 2013; Zahn et al., 2019).

3.2. TP identification

TP identification was performed as described in 2.3 and 2.4, by batch experiments where single-stage HRMS data was used to propose molecular formulas of the TPs based on mass accuracy and isotopic profile. As compiled in Tables 1 and 2, up to 5 and 7 TPs were detected for VP and PPE, respectively, and their empirical formula could be assigned with a high level of certainty (mass error below ±0.6 mDa and scores higher than 98). TPs are named with the abbreviation of their precursor compound and the nominal masses of the observed $[M+H]^+$ ion. Then structures (compiled in Figs. 1 and 3) were proposed based on MS/MS experiments (spectra and chromatograms shown in Figs. 2, 4, S3, S5, S6, S7), which are discussed below.

3.2.1. VP

Five TPs were detected for VP, 2 of them are proposed to be formed by oxidation of the vinylic side chain (i.e. VP-116 and VP-132), one by hydrolysis (VP-86) and the two remaining by dimerization reactions (VP-219 and VP-227), as presented in Fig. 1.

VP-86, i.e. 2-pyrrolidone, was also observed as the only detectable

Table 1
Summary of LC-QTOF formula assignment for VP TPs.

Compound	Experimental *m/z*	Molecular formulae	Error (mDa)	DBE	Score (%)
VP	*112.0759*	*C6 H9 N O*	*0.21*	*3*	*99.70*
VP-86	86.0605	C4 H7 N O	0.46	2	99.98
VP-116	116.0706	C5 H9 N O2	<0.01	2	99.99
VP-132	132.0661	C5 H9 N O3	0.58	2	99.98
VP-219	219.1602	C12H18 N4	−0.22	6	99.77
VP-227	227.1391	C11H18 N2 O3	0.08	4	99.97

Table 2
Summary of LC-QTOF formula assignment for PPE TPs.

Compound	Experimental *m/z*	Molecular formulae	Error (mDa)	DBE	Score (%)
PPE	*130.1336*	*C6 H15 N3*	*−0.27*	*1*	*100.00*
PPE-87	87.0913	C4 H10 N2	−0.37	1	98.93
PPE-111	111.0917	C6 H10 N2	0.03	3	100.00
PPE-115	115.0867	C5 H10 N2 O	0.11	2	99.92
PPE-126	126.1023	C6 H11 N3	−0.27	3	99.51
PPE-144	144.1127	C6 H13 N3 O	−0.44	2	98.85
PPE-146	146.1286	C6 H15 N3 O	−0.19	1	99.79
PPE-160	160.1076	C6 H15 N3 O2	0.45	2	98.84

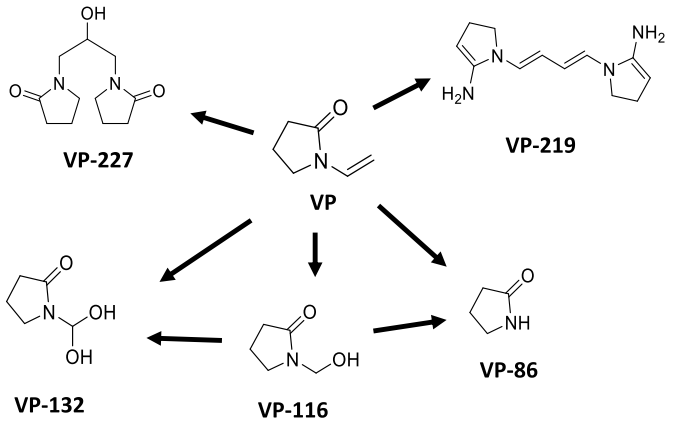

Fig. 1. Summary of VP TPs.

TP during hydrolysis experiments of VP by Zahn et al. (2019). Obviously, this TP was thus easy to identify as being expected and because of the MS/MS spectrum (Fig. S3b), that exhibits the loss of ammonia (in agreement with the observations of Zahn et al.) and other smaller product ions, consistent with that structure. Also, the spectrum matched well with that available in the METLIN library (MID 6452).

VP-116 and VP-132 are proposed to be formed as a result of the oxidation of the vinyl moiety, leading to mono- or di-hydroxylated species (Fig. 1). VP-116 spectrum displays only the loss of water and CO to yield *m/z* 70 (nominal masses are used in the text for conciseness), Fig. S3c. Similarly, VP-132 spectrum (Fig. 2a) also shows the same loss to yield *m/z* 86 in this case. Then a loss of ammonia to produce *m/z* 69 or C_2H_4O to yield *m/z* 42 is observed. Both *m/z* 86 and *m/z* 69 are also present in VP spectrum (Fig. S3a), which would confirm that the reaction takes place in the vinylic chain.

VP-219 would be produced as a result of the dimerization of VP and substitution of the two CO groups by amino groups. Dimerization is a reaction expected for VP, given that such compound is used as monomer in the production of VP-polymers. Although the introduction of N in the structure is not very intuitive, its spectrum (Fig. 2b) clearly shows a first loss of one 2-iminopyrrolidine group, followed by loss of ammonia (*m/z* 135 and *m/z* 118, respectively). In this case, *m/z* 85, corresponding to 2-iminopyrrolidine, is also observed, which then losses ammonia to yield *m/z* 68.

Finally, VP-227 would result from the dimerization of VP and either VP-116 or VP-132. Its spectrum (Fig. S3d) exhibits mainly two peaks, *m/z* 124, which would be formed as the result of the loss of a pyrrolidone moiety and water or *m/z* 104 related to the central alkyl group.

From Fig. S4, which summarizes the evolution of these TPs along time up to 1 h of irradiation, it is evident that dimeric TPs (particularly VP-219) were formed initially and further degraded. Furthermore, at longer periods, VP-116 is by far the most intense TP. Assuming its LC-MS response would be equal to that of VP, it would represent about a 50% yield. Indeed, this is only a conjecture based on the available data and actual yields could be calculated only if standards would be available, but helps in understanding the relative relevance of each TP.

3.2.2. PPE

As presented in Table 2 and Fig. 3, a total of 7 TPs were detected in the case of PPE, from which, one is a hydrolytic product (PPE-87) and the remaining are proposed to be formed by a dehydrogenation mechanism (PPE-126), which is then followed by either oxidative cleavage of the ethenamine group (PPE-111 and PPE-115) or oxidation of the piperazine cycle (PPE-144, PP-146 and PPE-160).

PPE-87, i.e. piperazine, was easily identified as the most logical structure and on the basis of its MS/MS spectrum (Fig. S5b), which also matches quite well the triple-quadrupole spectra available in MassBank (e.g. records KO003735 and KO003736).

From the remaining TPs, PPE-160 was also observed as the only sunlight photolytic product of PPE by Zahn et al. who also detected it, as well as PPE-126 as a TP from oxidation reactions in the presence of MnO_2 (Zahn et al., 2019). The MS/MS spectra obtained in our work (Figs. S5d and S5f) fit well with that described in that publication, so the same structures are proposed. Zahn et al. also detected a TP with nominal *m/z* 142 as a product in MnO_2 reaction. Such TP was not observed for UV photolysis, but in turn we observed PPE-144 and PPE-146. The spectrum of PPE-144 (Fig. 4b) shows different pathways involving either a loss of water or CH_3O, which could be compatible with a keto group, due to keto-enolic equilibrium. Thus, the structure shown in Fig. 3 is proposed, which would be similar to the TP with *m/z* 142 detected by Zahn et al. but without posing an unsaturation in the ethenamine group. Similarly, PPE-146 is proposed as hydroxylated PPE, given the fact that the first product ion (*m/z* 103, Fig. S5e) would correspond to the loss of the ethenamine group.

PPE-111 and PPE-115 are proposed to be oxidative cleavage products (Fig. 3). PPE-111 was assigned to the structure suggested in Fig. 3, given the loss of C_2H_4 observed in the spectrum (Fig. 4a), which would correspond to the ethene group in the structure. In the case of PPE-115, its spectrum (Fig. S5c) exhibits the loss of either CO or water, related again to a keto group. This keto group could be also present in the ring, but its location in the alkyl chain is more probable, due to its formation through an oxidative mechanism, similar to PPE-111. The transformation pathway presented in Fig. 3 assumes the formation of 2 further dehydration TPs, which were not detected, by analogy with PPE-126 and the reaction mechanism proposed by Zahn et al. for MnO_2 (Zahn et al., 2019).

As shown if Fig. S4b, the most relevant TP in terms of intensity is PPE-126, followed by PPE-87 and PPE-144.

3.3. Predicted toxicity

The prediction of VP, PPE and their TPs (eco)toxicities were performed both with US EPA T.E.S.T. and ECOSAR software. Data are compiled in Table S3 (T.E.S.T.) and Table S4 (ECOSAR; note that two toxicity values are predicted for some TPs depending on the functional groups class used to generate them). Furthermore, these data are also depicted in Fig. 5, where toxicological endpoints for TPs are compared to that of their parent chemicals, so that red colors indicate a lower predictable effect concentration (i.e. higher toxicity). It is evident from that data that each software leads to different results, as observed previously for diazepam TPs (Carpinteiro et al., 2017), and these toxicity estimations should be taken with caution.

Regarding VP, both software tools agreed that among its TPs, VP-219 is the only one that would result into a higher ecotoxicological concern, since it could be up to 100 times more toxic to daphnid species in chronic exposure (Fig. 5). However, as mentioned above, such compound appears to be an intermediate TP, whereas the most intense, VP-116 would be less ecotoxic than VP itself. Also, the oral rat predicted toxicity for this TP would be similar to VP, so the human risk should be maintained at a similar level. In all cases, predicted oral rat acute toxicity values fall in the 300–2000 mg/kg body weight range or higher, so they would

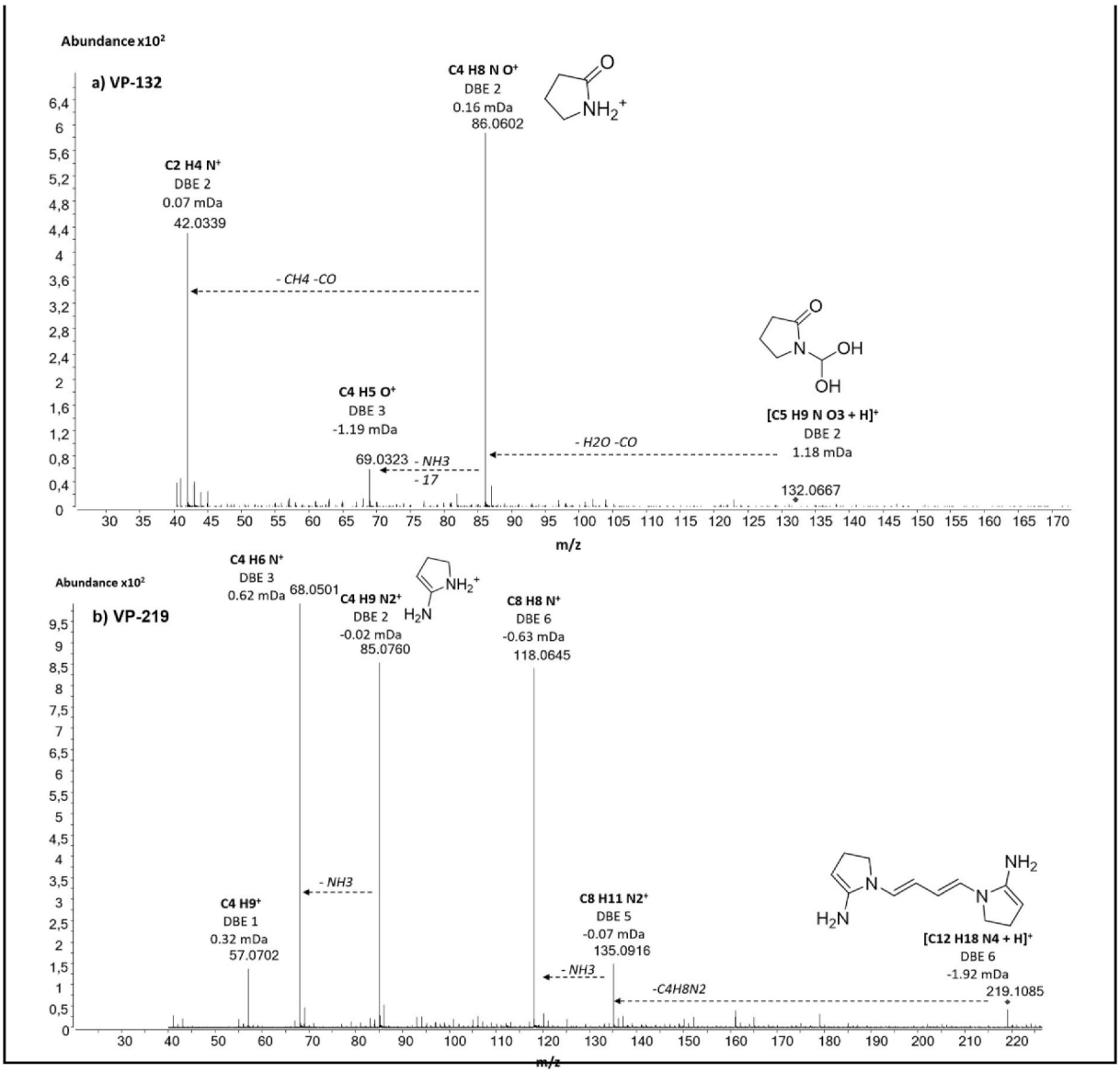

Fig. 2. MS/MS spectra of selected VP TPs (the remaining TP spectra are compiled in Figure S3).

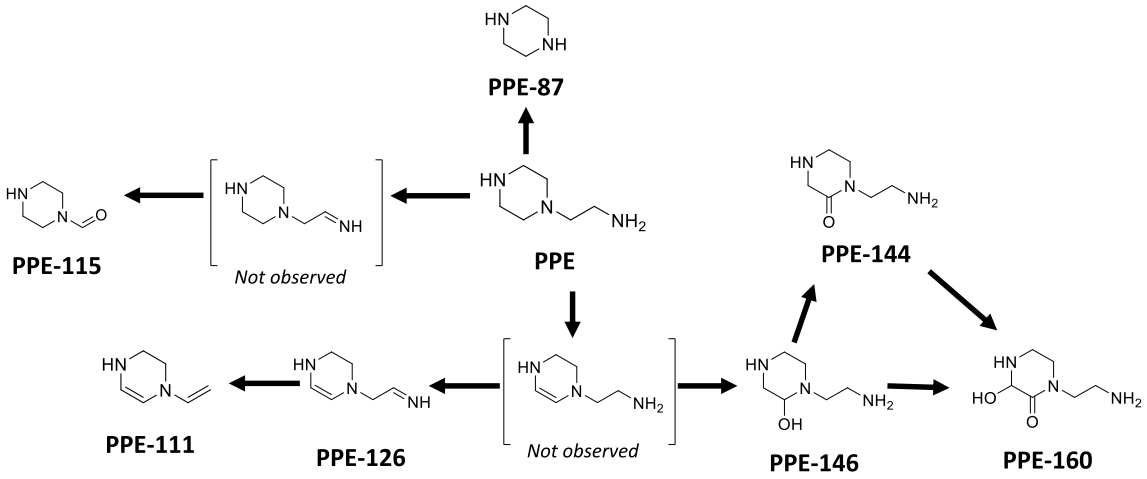

Fig. 3. Summary of PPE TPs.

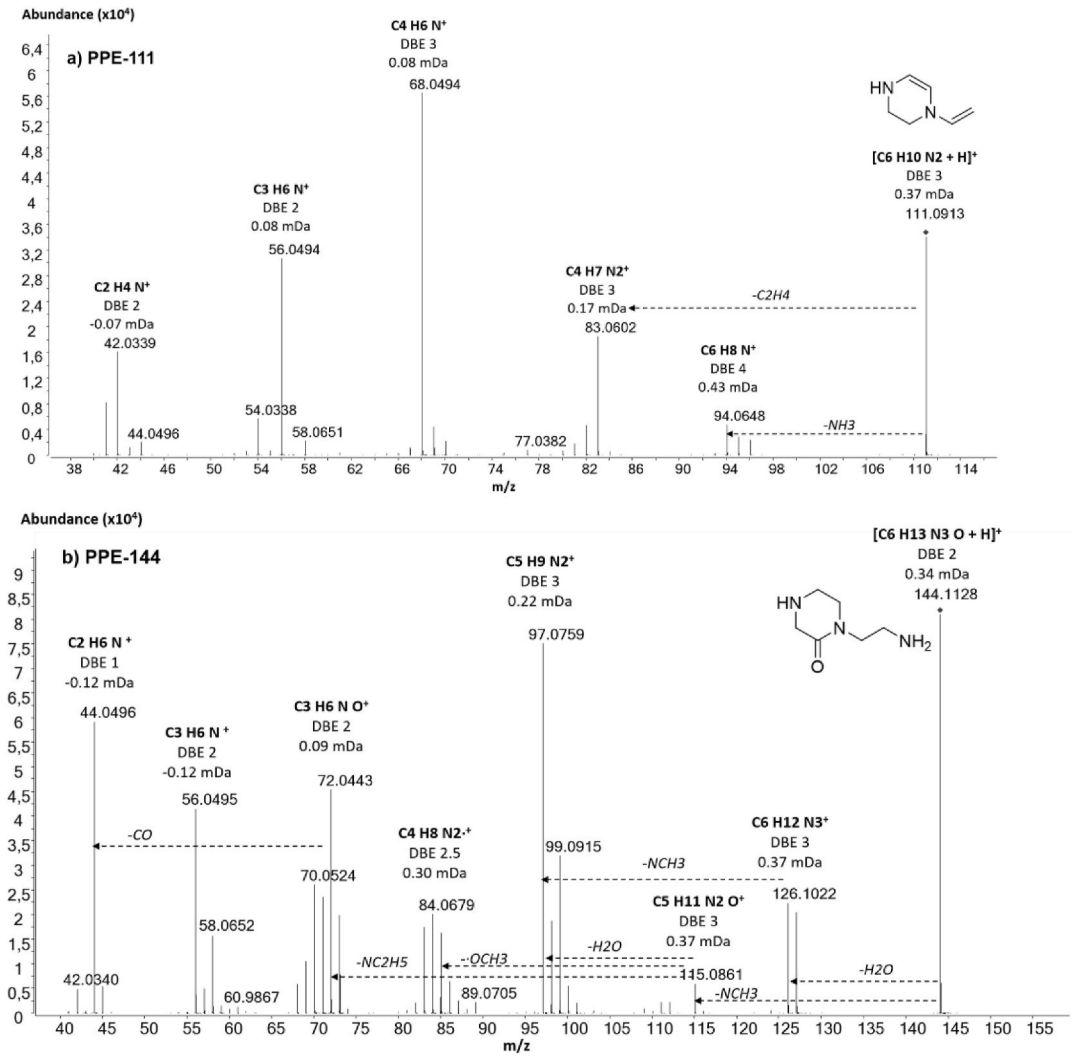

Fig. 4. MS/MS spectra of selected PPE TPs (the remaining TP spectra are compiled in Figure S5).

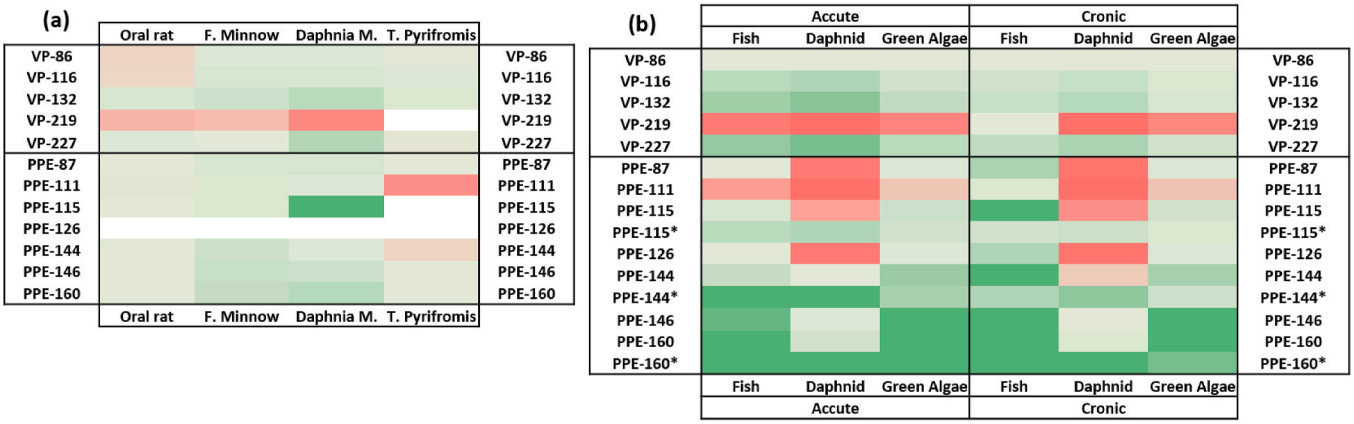

Fig. 5. Heatmaps of (eco)toxicological predicted data. (a): T.E.S.T. prediction. (b): ECOSAR prediction. Color code: From dark green (less toxic than parent chemical) to dark red (more toxic than parent chemical); White color refers to values that could not be predicted by T.E.S.T.. Detailed predicted toxicity values are compiled in Tables S2 and S3. When two ECOSAR values were provided for the same T, the symbol (*) corresponds to the prediction based on the "amide" group class, while the other estimation refers to "aliphatic amine" group class. (For interpretation of the references to color in this figure legend, the reader is referred to the Web version of this article.)

classify in Category 4 or "non-toxic" according to the ECHA Guidance (ECHA, 2017), thus human risk is expected to be low. Applying the same guidance document, all the TPs would classify as non-acute toxic (all acute toxicity endpoints are >1 mg/L), while chronic toxicity evaluation would require more robust data, even for screening purposes.

In the case of PPE, most TPs are not expected to be more toxic to rat

than PPE (Fig. 5) and according to their predicted values they would also classify in Category 4 or non-toxic, therefore likely not being hazardous for human health. In ecotoxicological terms PPE-111 seems to be the most concerning one, although predicted values differ among both QSAR tools and the yield of formation of this TP is very low (Fig. S4b). On the other hand, the most intense TP is PPE-126 (Fig. S4b), but its toxicity could not be predicted by T.E.S.T., while ECOSAR foreseen values are more relevant in the case of daphnid species. Even so, the predicted acute toxicological endpoints are >1 mg/L, thus acute ecotoxic effects would not be expected. Thus far, an experimental ecotoxicological evaluation would be required to confirm these findings.

4. Conclusions

The investigated high-volume production chemicals VP and PPE significantly reacted with UV radiation. These two chemicals lead to the formation of a wide range of TPs, that could be potentially formed during advanced water treatment and in surface waters. Twelve TP were found for both substances as products of oxidation, hydrolysis and dimerization reactions, being the dehydrogenation product PPE-126 and the oxidation of vinyl moiety VP-116, the most abundant TP of PPE and VP, respectively. The degradation of VP occurs much faster ($t_{1/2}$ lower than 2 min), than in the case of PPE, which degradation $t_{1/2}$ approaches half an hour. A preliminary QSAR screening of their potential toxicological implications point to a low environmental and human hazard of the TP. A further comprehensive evaluation of hazard assessment of both parent compounds and transformation products can be performed as proposed by Zheng et al. (Zheng et al., 2021) for decabromodiphenyl ether, and its alternatives and with experimental data, particularly in a chronic exposure basis.

Credit author statement

B.J. Sieira: Investigation, R. Rodil: Conceptualization, Data curation, Formal analysis, Supervision & Writing – review & editing. R. Cela: Supervision & Resources, J.B. Quintana: Conceptualization, Data curation, Formal analysis, Supervision, Funding acquisition adquisition & Writing – review & editing, R. Montes: Investigation, Data curation, Writing – original draft, Writing – review & editing.

Declaration of competing interest

The authors declare that they have no known competing financial interests or personal relationships that could have appeared to influence the work reported in this paper.

Acknowledgments

This work was supported by the Water Challenges for a Changing World Joint Program Initiative (Water JPI) Pilot Call (ref. WATER-JPI2013 – PROMOTE), funded by the Spanish Ministry of Economy and Competitiveness/Spanish Agencia Estatal de Investigación (refs. JPIW 2013-117, CTM2017-84763-C3-2-R and PID2020-117686RB-C32). We also acknowledge the Galician Council of Culture, Education and Universities (ref. ED431C2021/06). This research has been co-financed by the European Regional Development Fund through the Interreg V-A Spain-Portugal Programme (POCTEP) 2014–2020 (ref. 0725_NOR_WATER_1_P). It only reflects the author's view; thus, Programme authorities are not liable for any use that may be made of the information contained therein.

Appendix A. Supplementary data

Supplementary data to this article can be found online at https://doi.org/10.1016/j.chemosphere.2021.132394.

References

Antić, V.V., Antić, M.P., Kronimus, A., Oing, K., Schwarzbauer, J., 2011. Quantitative determination of poly(vinylpyrrolidone) by continuous-flow off-line pyrolysis-GC/MS. J. Anal. Appl. Pyrolysis 90 (2), 93–99. https://doi.org/10.1016/j.jaap.2010.10.011.

Arp, H.P.H., Brown, T.N., Berger, U., Hale, S.E., 2017. Ranking REACH registered neutral, ionizable and ionic organic chemicals based on their aquatic persistency and mobility. Environ Sci Process Impacts 19 (7), 939–955. https://doi.org/10.1039/C7EM00158D.

Bieber, S., Greco, G., Grosse, S., Letzel, T., 2017. RPLC-HILIC and SFC with mass spectrometry: polarity-extended organic molecule screening in environmental (water) samples. Anal. Chem. 89 (15), 7907–7914. https://doi.org/10.1021/acs.analchem.7b00859.

Bletsou, A.A., Jeon, J., Hollender, J., Archontaki, E., Thomaidis, N.S., 2015. Targeted and non-targeted liquid chromatography-mass spectrometric workflows for identification of transformation products of emerging pollutants in the aquatic environment. Trac. Trends Anal. Chem. 66, 32–44. https://doi.org/10.1016/j.trac.2014.11.009.

Carpinteiro, I., Rodil, R., Quintana, J.B., Cela, R., 2017. Reaction of diazepam and related benzodiazepines with chlorine. Kinetics, transformation products and in-silico toxicological assessment. Water Res. 120, 280–289. https://doi.org/10.1016/j.watres.2017.04.063.

Castro, G., Casado, J., Rodríguez, I., Ramil, M., Ferradás, A., Cela, R., 2016. Time-of-flight mass spectrometry assessment of fluconazole and climbazole UV and UV/H2O2 degradability: kinetics study and transformation products elucidation. Water Res. 88, 681–690. https://doi.org/10.1016/j.watres.2015.10.053.

Chemicalize, 2021. https://chemicalize.com/app/calculation/C1CN(CCN1)CCN.

European Chemicals Bureau, 2003. European Union Risk Assessment Report. 1-Vinyl-2-Pyrrolidone, vol. 39. 2nd priority List from. https://echa.europa.eu/documents/10162/1ebf6d5f-e907-4ca2-a3b4-909fd5f359d1. (Accessed 16 May 2021).

ECHA, 2010. 2-piperazin-1-ylethylamine ECHA Registration Dossier. Retrieved 16/03/2021, from. https://echa.europa.eu/es/registration-dossier/-/registered-dossier/16054/1/2.

ECHA, 2011. 1-vinyl-2-pyrrolidone ECHA Registration Dossier. Retrieved 16/03/2021, from. https://echa.europa.eu/registration-dossier/-/registered-dossier/15035/1.

ECHA, 2017. Guidance on the Application of the CLP Criteria. Retrieved 16/03/2021, from. https://www.echa.europa.eu/documents/10162/13562/clp_en.pdf/58b5dc6d-ac2a-4910-9702-e9e1f5051cc5.

European Environment Agency, 2019. The European Environment-State and Outlook 2020 Knowledge for Transition to a Sustainable Europe. Retrieved 16/05/2021, from https://www.eea.europa.eu/publications/soer-2020.

Gago-Ferrero, P., Schymanski, E.L., Bletsou, A.A., Aalizadeh, R., Hollender, J., Thomaidis, N.S., 2015. Extended suspect and non-target strategies to characterize emerging polar organic contaminants in raw wastewater with LC-HRMS/MS. Environ. Sci. Technol. 49 (20), 12333–12341. https://doi.org/10.1021/acs.est.5b03454.

González-Mariño, I., Rodríguez, I., Rojo, L., Cela, R., 2018. Photodegradation of nitenpyram under UV and solar radiation: kinetics, transformation products identification and toxicity prediction. Sci. Total Environ. 644, 995–1005. https://doi.org/10.1016/j.scitotenv.2018.06.318.

Hale, S.E., Arp, H.P.H., Schliebner, I., Neumann, M., 2020. What's in a name: persistent, mobile, and toxic (PMT) and very persistent and very mobile (vPvM) substances. Environ. Sci. Technol. 54 (23), 14790–14792. https://doi.org/10.1021/acs.est.0c05257.

Helbling, D.E., Hollender, J., Kohler, H.-P.E., Singer, H., Fenner, K., 2010. High-throughput identification of microbial transformation products of organic micropollutants. Environ. Sci. Technol. 44 (17), 6621–6627. https://doi.org/10.1021/es100970m.

Hu, X., Ji, H., Wu, L., 2012. Singlet oxygen photogeneration and 2,4,6-TCP photodegradation at Pt/TiO2 under visible light illumination. RSC Adv. 2 (32), 12378–12383. https://doi.org/10.1039/C2RA21661B.

Kern, S., Fenner, K., Singer, H.P., Schwarzenbach, R.P., Hollender, J., 2009. Identification of transformation products of organic contaminants in natural waters by computer-aided prediction and high-resolution mass spectrometry. Environ. Sci. Technol. 43 (18), 7039–7046. https://doi.org/10.1021/es901979h.

Montes, R., Aguirre, J., Vidal, X., Rodil, R., Cela, R., Quintana, J.B., 2017. Screening for polar chemicals in water by trifunctional mixed-mode liquid chromatography–high resolution mass spectrometry. Environ. Sci. Technol. 51 (11), 6250–6259. https://doi.org/10.1021/acs.est.6b05135.

Montes, R., Rodil, R., Cela, R., Quintana, J.B., 2019. Determination of persistent and mobile organic contaminants (PMOCs) in water by mixed-mode liquid chromatography–tandem mass spectrometry. Anal. Chem. 91 (8), 5176–5183. https://doi.org/10.1021/acs.analchem.8b05792.

Neumann, M., 2017. Protecting the Sources of Our Drinking Water. A Revised Proposal for Implementing Criteria and an Assessment Procedure to Identify Persistent, Mobile and Toxic (PMT) and Very Persistent, Very Mobile (VPvM) Substances under REACH.

Reemtsma, T., Berger, U., Arp, H.P.H., Gallard, H., Knepper, T.P., Neumann, M., Quintana, J.B., Voogt, P.d., 2016. Mind the gap: persistent and mobile organic compounds—water contaminants that slip through. Environ. Sci. Technol. 50 (19), 10308–10315. https://doi.org/10.1021/acs.est.6b03338.

Ryu, J., Monllor-Satoca, D., Kim, D.-h., Yeo, J., Choi, W., 2013. Photooxidation of arsenite under 254 nm irradiation with a quantum yield higher than unity. Environ. Sci. Technol. 47 (16), 9381–9387. https://doi.org/10.1021/es402011g.

Schulze, S., Sättler, D., Neumann, M., Arp, H.P.H., Reemtsma, T., Berger, U., 2018. Using REACH registration data to rank the environmental emission potential of persistent and mobile organic chemicals. Sci. Total Environ. 625, 1122–1128. https://doi.org/10.1016/j.scitotenv.2017.12.305.

Schulze, S., Zahn, D., Montes, R., Rodil, R., Quintana, J.B., Knepper, T.P., Reemtsma, T., Berger, U., 2019. Occurrence of emerging persistent and mobile organic contaminants in European water samples. Water Res. 153, 80–90. https://doi.org/10.1016/j.watres.2019.01.008.

Schymanski, E.L., Singer, H.P., Longrée, P., Loos, M., Ruff, M., Stravs, M.A., Ripollés Vidal, C., Hollender, J., 2014. Strategies to characterize polar organic contamination in wastewater: exploring the capability of high resolution mass spectrometry. Environ. Sci. Technol. 48 (3), 1811–1818. https://doi.org/10.1021/es4044374.

Sieira, B.J., Montes, R., Touffet, A., Rodil, R., Cela, R., Gallard, H., Quintana, J.B., 2020. Chlorination and bromination of 1,3-diphenylguanidine and 1,3-di-o-tolylguanidine: kinetics, transformation products and toxicity assessment. J. Hazard Mater. 385, 121590. https://doi.org/10.1016/j.jhazmat.2019.121590.

Weidauer, C., Davis, C., Raeke, J., Seiwert, B., Reemtsma, T., 2016. Sunlight photolysis of benzotriazoles – identification of transformation products and pathways. Chemosphere 154, 416–424. https://doi.org/10.1016/j.chemosphere.2016.03.090.

Wols, B.A., Hofman-Caris, C.H.M., 2012. Review of photochemical reaction constants of organic micropollutants required for UV advanced oxidation processes in water. Water Res. 46 (9), 2815–2827. https://doi.org/10.1016/j.watres.2012.03.036.

Zahn, D., Mucha, P., Zilles, V., Touffet, A., Gallard, H., Knepper, T.P., Frömel, T., 2019. Identification of potentially mobile and persistent transformation products of REACH-registered chemicals and their occurrence in surface waters. Water Res. 150, 86–96. https://doi.org/10.1016/j.watres.2018.11.042.

Zheng, Z., Arp, H.P.H., Peters, G., Andersson, P.L., 2021. Combining in silico tools with multicriteria analysis for alternatives assessment of hazardous chemicals: accounting for the transformation products of decaBDE and its alternatives. Environ. Sci. Technol. 55 (2), 1088–1098. https://doi.org/10.1021/acs.est.0c02593.